Surface Micromachined Polysilicon Heart Cell Force Transducer

Gisela Lin, *Member, IEEE*, Kristofer S. J. Pister, and Kenneth P. Roos

Abstract—A microelectromechanical systems (MEMS) force transducer system, with a volume less than 1 mm^3 millimeter, has been developed to measure forces generated by living heart muscle cells. Cell attachment and measurement of contractile forces have been demonstrated with a commercially fabricated surface-micromachined hinged polysilicon device. Two freestanding polysilicon clamps, each suspended by a pair of microbeams, hold each end of a heart cell. When the cell contracts, the beams bend and force is determined from the measured deflection and the spring constant in the beams. The average maximal force over seven contractile experiments using a calcium solution stimulus was $F_{\max} = 12.6 \pm 4.66$ μN. Normalizing to a cross-sectional area, $F_{\max}$/area was 23.7$\pm$8.6 mN/mm^2. These force data were also correlated to optically imaged striation pattern periodicity. Intermediate forces were also measured in response to a calcium solution gradient and showed similar behavior to those measured in other laboratories. This MEMS force transducer demonstrates the feasibility of higher fidelity measurements from muscle cells and, thus, an improved understanding of the mechanisms of muscle contraction. [389]

Index Terms—Force transducer, heart cell, hinged microstructures, MEMS, micromechanical, surface micromachining.

I. INTRODUCTION

FORCE measurements from cardiac muscle have generally been restricted to multicellular tissue and whole organ preparations due to their relative durability and ease of interfacing to standard force or pressure transducers [1], [2]. Attempts to scale systems down to the smaller single ventricular cell (cardiac myocyte) level has proven problematic with standard commercial transducer technology [2]–[9]. Such devices, capable of force measurement in the millinewton range, are massive (on the order of 50–100 g) relative to a single cell and must be positioned outside the cell's saline bath. These physical constraints necessitate complex cell transducer interfaces that are of high mass relative to the cell and inherently exhibit compliance and drift. These experimental design characteristics limit the frequency response and increase the noise levels well above manufacturer's specifications. Additionally, attachment structures must enter the bath and are subject to surface tension forces that can be greater than that of the cell's force. Thus, force readings may be subject to ambiguous artifacts, be difficult to interpret, and are limited to frequency ranges typically no greater than 100 Hz when cells are attached.

Microelectromechanical systems (MEMS) technology offers the ability to shrink the force transducer down to a size comparable to that of a cardiac myocyte. The fabrication of three-dimensional (3-D) MEMS microstructures permit the simplification of the entire device including the cell attachment interface. Thus, the entire miniaturized device can be placed into the cell's bath, eliminating the need to traverse the air/bath interface. Although there are several laboratories working towards characterizing mechanical function from cardiac myocytes, none are using MEMS technology. At a subcellular level, Fauver *et al.* [10] have reported the use of a silicon–nitride cantilever device to perform force measurements on isolated muscle protein filaments. However, MEMS technology has not previously been used to evaluate mechanical function from muscle cell preparations.

To study the contractile properties of heart cells, such as the kinetic changes in the molecular motor proteins of the cell, a mechanical bandwidth in the kilohertz range is desirable with forces resolved from the 50 nN to 50 μN range. The ends of the cell must be firmly attached to the transducer to prevent slippage during a contraction, and transmitted light illumination through the cell is highly desirable to visually monitor the microscopic changes in protein distribution throughout the cell during a contraction. A fully submersible miniaturized polysilicon force transducer less than (1 mm^3) has been designed that meets these criteria and eliminates surface tension artifacts. With this low mass transducer, steady-state measurements of direct force from single heart cells have been made. This device also demonstrates the feasibility of dynamic measurements such as the complex stiffness modulus and length or force transients from isolated heart cells with a bandwidth in excess of 1 kHz.

II. THEORY

Fig. 1 shows the device's principle of operation. A single heart cell was glued between two polysilicon clamps, and the clamps moved towards each other in response to the cell's contraction. Based on the amount of cell shortening, force was estimated using $F = kx$ where $k =$ the spring constant in the beams and $x =$ half the total cell shortening, assuming the clamp displacement in response to the cell's contraction is equal on both sides.

G. Lin is with the Microelectromechanical Technology Group, Jet Propulsion Laboratory, California Institute of Technology, Pasadena, CA 91109-8099 USA (e-mail: Gisela.Lin@jpl.nasa.gov).

K. S. J. Pister is with the Berkeley Sensor and Actuator Center, University of California at Berkeley, Berkeley, CA 94720-1770 USA.

K. P. Roos is with the Cardiovascular Research Laboratory, Department of Physiology, University of California at Los Angeles (UCLA) School of Medicine, University of California at Los Angeles, Los Angeles, CA 90095-1760 USA.
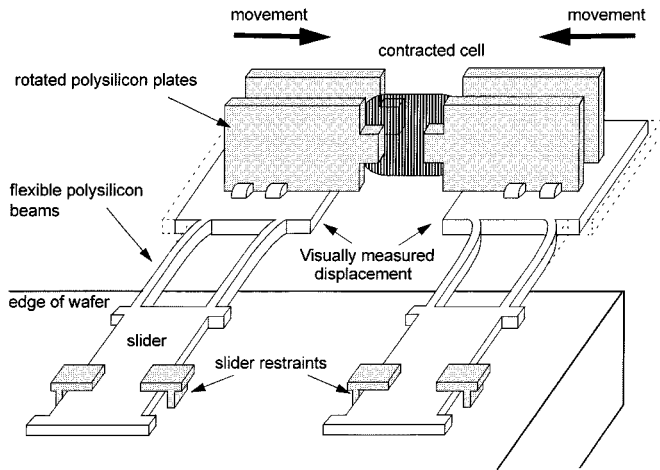
Fig. 1.   Schematic diagram of the principle of operation for this device. When the cell contracts, the beams bend and the amount of cell shortening is optically determined. Force is estimated by taking half the total shortening and multiplying this value by the effective spring constant in the beams.

Theoretically, the spring constant of a single fixed free cantilever beam, deflected sideways, is described by

$$k(a, b, L) = \frac{ab^3 E}{4L^3} \tag{1}$$

where a is the beam thickness $= 2\ \mu m$, b is the beam width $= 4\ \mu m$, L is the beam length $= 200\ \mu m$, and E is the elastic modulus of the polysilicon. The two beams attached to each clamp should have a combined spring constant eight times that of a single beam. Since the beams were in a clamped–clamped configuration rather than a clamped-free single-beam configuration, the single-beam spring constant was multiplied by a factor of four. An added factor of two comes from the fact that there are two beams.

In terms of the physiological aspects, heart cells differ in size and shape, with most cells 100–150-μm long and 15–30-μm wide. The measured maximal force generated by each cell must be normalized to the cross-sectional area of the cell in order to compare the force generating performance between cells of differing size. Thus, the contractile force generation capability can be quantified independent of cell size. As a first-order approximation, the cross section of the muscle cell was estimated as an ellipse with a major axis to minor axis ratio of 1.25 : 1 [6]. The area of the cell cross section was then

$$A = (1.25)\pi \left(\frac{w}{2}\right)^2 \tag{2}$$

where w is the measured width of the cell.

The cells used in these experiments were demembranated ("skinned"), Thus, calcium ions were necessary to activate the contractile proteins and initiate force production. Force levels are modulated by varying the amount of calcium ion exposed to the cell. The concentration of calcium (Ca^{2+}) can vary over several orders of magnitude and is usually expressed in terms

of pCa ($pCa = -\log_{10}[Ca^{2+}]$). The sigmoidal force-pCa relationship can be theoretically described by a "Hill curve" as in the following equation:

$$\% \max force = \frac{F}{F_{max}} \times 100$$
$$= \frac{100}{1 + 10^{\left[n_H(pCa - pCa_{50})\right]}} \tag{3}$$

where n_H represents the maximum slope of the curve and pCa_{50} is the calcium concentration where 50% of maximum activation is achieved. Both n_H and pCa_{50} are routinely used to compare muscle force-pCa characteristics under different conditions or cell types [2]–[5], [8].

Muscle cells are composed of interdigitating filaments primarily consisting of the contractile proteins actin and myosin. The filament overlap is highly regular such that a lengthwise cross section of a muscle cell appears striated with dark and light bands. These bands form the striations seen in "striated muscle" and are organized into "sarcomeres," which span the length of the heart cell. Striation pattern periodicity or the sarcomere length is directly related to the degree of contractile protein interdigitation and, thus, the amount of force generated by the cell [2].

III. METHODS

A. Design Considerations

The force transducer was fabricated using the multiuser MEMS processes (MUMP's) at Cronos Integrated Microsystems Inc., Morrisville, NC.[1] This process offers two polysilicon structural layers separated by two sacrificial oxide layers. By strategically patterning and connecting the polysilicon layers, 3-D mechanical components such as scissor hinges and spring locks were created [11]. Earlier designs have been described in the literature [12] and [13]. Fig. 2 shows an SEM photograph of the current design. A heart cell was glued between the polysilicon clamps using a silicone sealant (Dow Corning silicone rubber sealant, Midland, MI). Each clamp was attached to a slider via two $200 \times 4 \times 2\ (\mu m)^3$ beams. These clamps were slid off the edge of the wafer using the sliders. Thus, the transmitted light illumination path was not blocked by the substrate to permit optical imaging of the entire cell and its contractile proteins. Fig. 3 shows a close-up of the left clamp, scissor hinge, spring lock, and flexible beams.

B. Microstructure Fabrication and Release Etching

Before release etching, each device was individually diced. The oxide separating the polysilicon layers was phosphosilicate glass (PSG) and was etched from underneath the polysilicon layers, freeing these layers and allowing them to move. The typical etchant was liquid 49% hydrofluoric acid (HF), which has a near infinite selectivity for oxide over polysilicon. Thus, the etching of polysilicon in HF was negligible.

When the chips came back from Cronos Integrated Microsystems, a protective layer of photoresist covered each die. After removing the chip's protective photoresist coating in acetone,
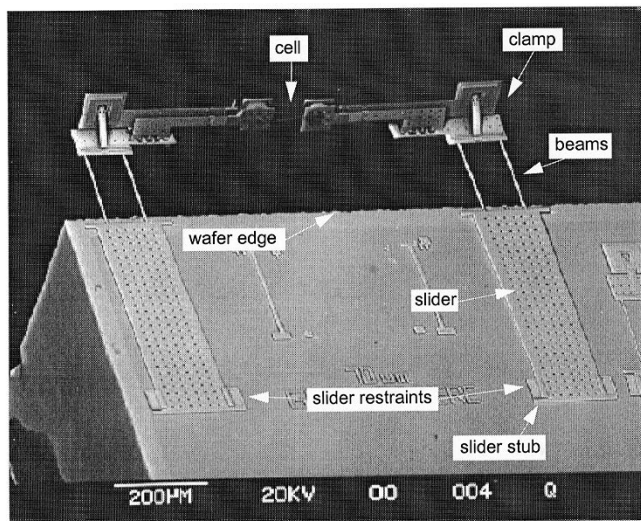
Fig. 2. SEM photograph of overhanging clamps. Clamps are composed of 1.5-μm-thick polysilicon plates, while the slider and beams are 2-μm-thick polysilicon. The ends of the slider have stubs that prevent the slider from sliding all the way out. When these stubs meet the restraint, the structure extends 300 μm past the wafer edge. A cell is glued between the clamps using a silicone sealant.
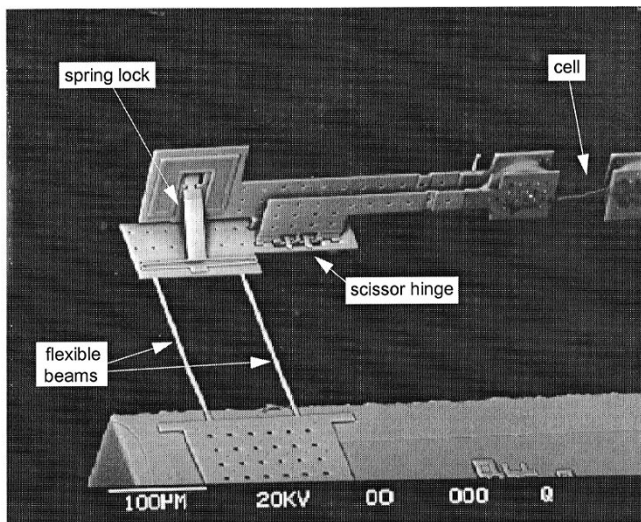

Fig. 3. Close-up of the left clamp shown in Fig. 2. Vertical plates are attached to a movable shuttle. Scissor hinges allow the vertical plates to rotate with respect to each other and translate in response to the cell's contraction. A spring lock supports the back vertical plate at 90°. The attachment sites on the vertical plates were 65 μm × 60 μm.

the chip was released in 49% HF for 1 min and 20 s, with agitation. Deionized (DI) water was used to rinse the chip before dipping it in methanol and allowing the chip to dry in air. This release method was very reliable. Other release methods such as critical point drying or surface assembled monolayers would also have been effective, but were not used.

C. Rat Heart Cell Preparation

The cells were prepared fresh each experimental day from adult rat ventricles subject to retrograde coronary artery perfusion (Langendorff) with 0.1% collagenase (Worthington Biochemical Corporation, Freehold, NJ, type 2) in Joklik
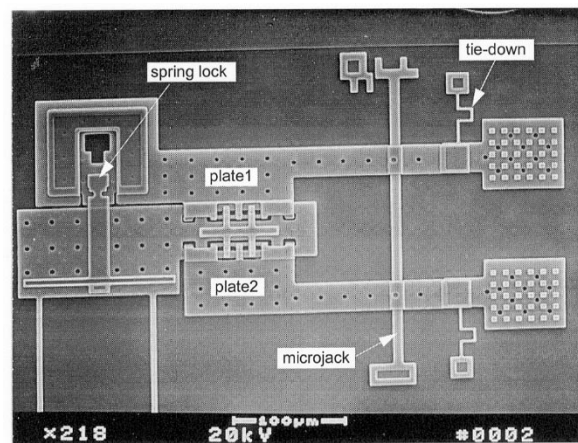

Fig. 4. SEM photo of unassembled clamp showing the two plates and spring locked hinges. The fixed-free beam is an assembly aid used to help lift the plates (microjack). Tie-downs are used to hold the structure flat after release and are broken as part of the assembly process.

minimum essential medium (Irvine Scientific, Irvine, CA) at 7.4 pH [5]. Following 10–20 min of perfusion, the cells were isolated by mincing and mechanically agitating the left ventricle in relaxing solution (see Section III-D). These cells were demembranated (skinned) for experiments by adding 1% ultra-pure Triton X-100 detergent to the relaxing solution for 20 min (Triton X-100, Sigma Chemical Company, St. Louis, MO). The cells were washed to remove any traces of detergent and attachment to the transducer began. All cells were used within the first 4 h after extraction on that experimental day to eliminate any possible cellular deterioration.

D. Relaxing and Activating Solution Preparation

The solutions used in these experiments were relaxing and activating solutions that contained the appropriate concentrations of salts, enzymes, and nutrients to keep the cells alive once they were extracted from the heart [5]. The relaxing solution has a pCa ≈ 8 ([Ca^{2+}] $\approx 10^{-8}$M). The maximal activating solution (pCa $= 4.5$, i.e., [Ca^{2+}] $= 10^{-4.5}$M), was made by adding 0.1-M CaCl to relaxing solution in the ratio 1 : 10. For example, 5 ml of 0.1-M CaCl (Ciba-Corning Diagnostic Corporation, Medfield, MA) was added to 50 ml of relaxing solution.

To acquire force-pCa data, a series of intermediate activating solutions between the maximal activating solution and the relaxing solution were made by mixing them in specific ratios to create solutions with pCa varying from 5.0 to 6.0 in steps of 0.2. Extra solutions were made for pCa $= 6.5$ and pCa $= 5.5$. These values for pCa were chosen based on the expected steep rise in force from around 10%–90% between pCa $= 5.0$ and pCa $= 6.0$ [5].

E. Assembly and Cell Attachment

All cell manipulation and microstructure assembly was done manually at a probe station using four sharp needle probes.[2] Fig. 4 shows an SEM photograph of an unassembled clamp. Two

(a)   (b)   (c)

Fig. 6. Diagram illustrating method of cell length adjustment. Clamps are rotated outwards about the slider restraint to take up cell slack before being glued down to the substrate.
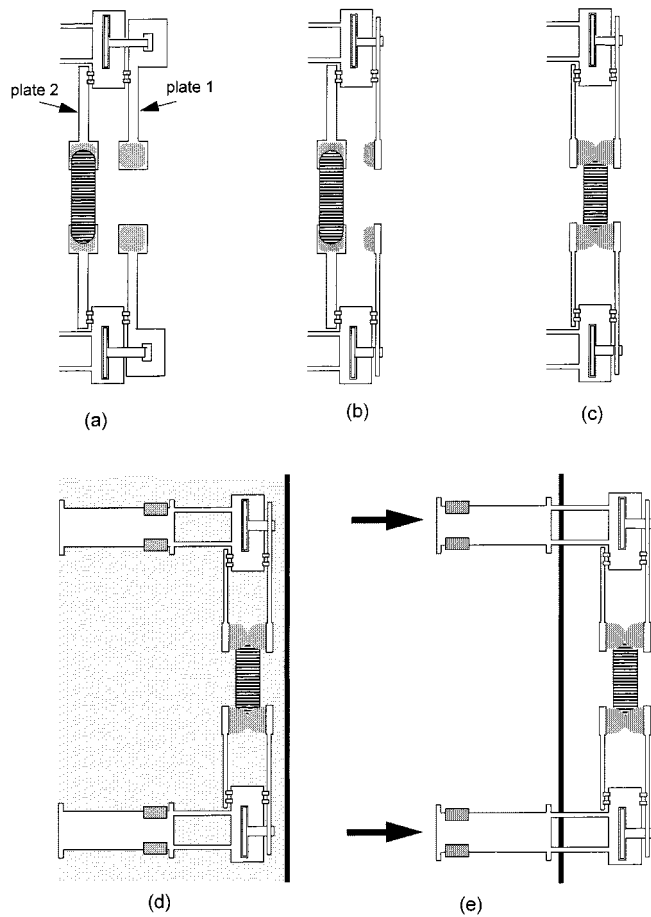

(d)   (e)

Fig. 5. Illustration of cell attachment and clamp assembly sequence. (a) First glue is applied to all four pads when the chip is dry. The cells in solution are then introduced and a cell of appropriate length is chosen and glued between the left pads. (b) The right pads are then rotated up 90° to the surface using metal probes and secured using the spring locks. (c) The left pads are then rotated, paying attention not to stretch or excessively deform the cell. The pair of pads on each clamp is pressed together to ensure a firm, complete seal around the ends of the cell. (d) The glue is allowed to set for approximately 30 min. (e) Finally, the clamps are simultaneously rolled off the edge of the wafer using metal probes.

manual assembly aides are shown—a fixed-free beam and corrugated beam. The fixed-free beam (also known as a "microjack") was buckled by pushing the free end towards the fixed end with a metal probe. The buckling caused the plates above it to lift upwards with enough height to allow a needle probe to slide under it reliably [14]. Thin corrugated polysilicon beams (also known as "tie-downs") prevented the plates from rotating upwards during the final rinse. These beams were meant to be broken as part of the device assembly process. Cell attachment occurred simultaneously with clamp assembly on the substrate.

Figs. 4 and 5 show the sequence of assembly and cell attachment steps. Starting with the chip mounted on a coverslip and placed in the experimental chamber (Section III-G) silicone sealant was applied to the surface of all four attachment sites when the clamps were dry and flat [see Fig. 5(a)]. The experimental chamber was then filled with relaxing solution. One drop of skinned cells was added to the chamber in a location away from the clamps to prevent unwanted cells getting stuck in the glue. Using metal probes, a cell of the proper length was selected and its ends were placed onto the attachment sites and glue on
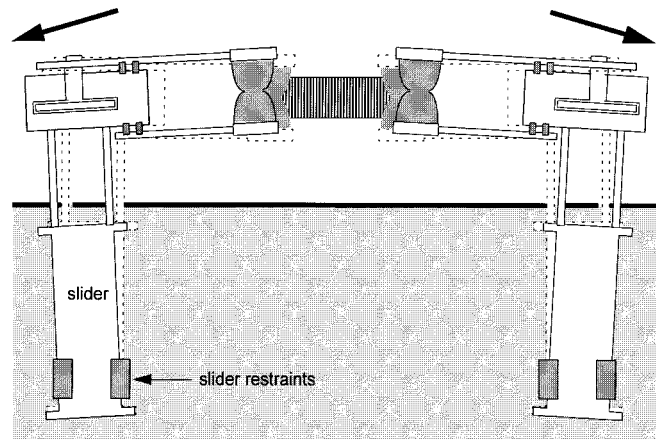
plate #2 of each arm. All the tie-downs were broken (Fig. 4) and a probe was used to buckle the microjack under one clamp arm. A second probe was slid under the top plate (#1). Plate #1 was rotated up and locked at 90° using the spring lock. The same procedure is repeated for the second clamp [see Fig. 5(b)]. To complete the cell attachment, the microjack under one clamp arm is again buckled by sliding a probe underneath plate #2. The other fixed-free beam is used to slide a separate probe under plate #2 of the second clamp. Both these plates (with the cell) are carefully rotated simultaneously until they meet the vertically locked plates #1 [see Fig. 5(c)]. The ends of the cell are secured by pressing each pair of attachment sites together for several minutes to make sure the glue coats the entire end. Finally, the clamps are pushed off the edge of the wafer [see Fig. 5(d) and (e)] with two probes, positioned at the edge of each slider. To minimize overstretching the cell, the sliders are simultaneously pushed slowly until the stubs on the end of the slider meet the restraints. After 30 min, the silicone sealant was set and contractile experiments begun.

F. Cell Length Adjustment

Often the cells would be slack after attachment, due to suboptimal cell positioning or glue expulsion after pressing attachment sites together. Taking up the slack was important in achieving a cell length for optimal force production. Earlier versions of this device did not have any cell length adjustment capability [15]. With this device design, the slack could be taken up by simply rotating the clamps outward about the slider restraints, as shown in Fig. 6. The slider restraints were only 56-μm long while the sliders were 560-μm long, so a rotation of a few degrees could take up sufficient slack. After rotation, the slider was glued down to the substrate using the silicone sealant applied underwater to prevent any slider movement during the cell contraction. The degree of cell slackness varied from cell to cell, and the sarcomere length could not be determined during assembly. However, the data indicated adequate adjustment (see Section IV). Although this method did not maintain perfect linearity of the cell position and direction of force generation, the amount of rotation was minimal. The clamp spacing at the start of each experiment was measured using image analysis
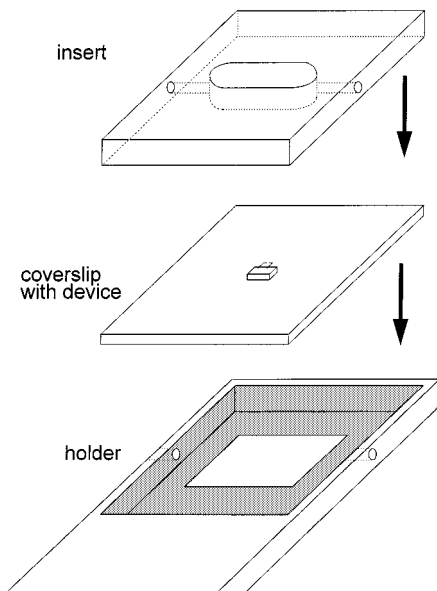
Fig. 7. Diagram of the custom-made holder and insert used with the chip during cell experiments. The holder has a square hole cut in the middle to allow transmitted light to pass through the cell. The coverslip fits into the square chamber in the holder. Cell attachment and transducer assembly takes place in this chamber. Afterwards, the insert fits over the transducer to convert the large square chamber into a small oval chamber with input and output solution lines.
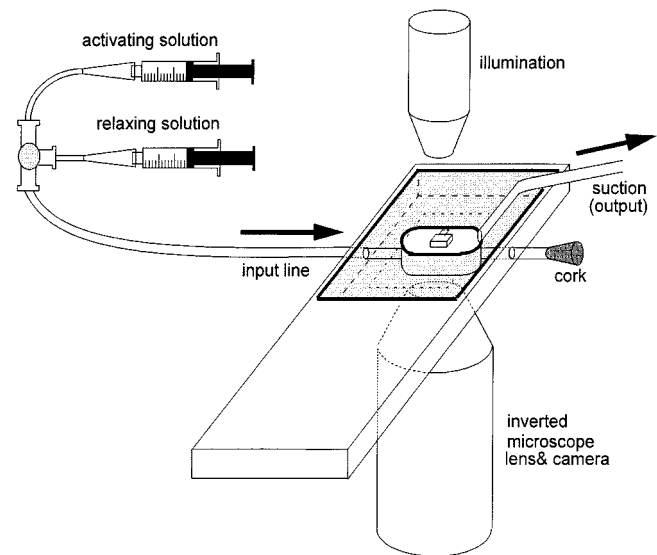

Fig. 8. Diagram of the test set-up. Holder sits on top of an inverted microscope lens with camera underneath to image the cell. Activating and relaxing solutions are pumped in manually through the input line. Instead of using the output line, a suction tube is placed at the top of the chamber to control the level of the solution meniscus.

(see below). Assuming the same amount of rotation in each clamp, there was at most 10 μm of outward movement in each clamp as a result of this adjustment (3–5 μm was typical). Ten micrometers is roughly 1% of the entire device length (beams + slider), thus, to first order the force generated by the cell was assumed to be in the direction normal to the beams.

G. Experimental Chamber

The experimental chamber was machined out of acrylic (Fig. 7). It consisted of a coverslip holder and insert that was designed to provide efficient solution exchanging by converting the large square chamber into a much smaller oval chamber with input and output solution lines. The size of the oval chamber was 2.5 mm $\times$ 7 mm $\times$ 1.5 mm and it held about 26 μl of liquid.

Since the oval chamber was so small, each device had to be individually diced to fit. Each device was used only once and then discarded. After dicing, each device was released using the method described above in Section III-B. Once dried, each device was then glued using 5-min epoxy to a glass coverslip (22 mm $\times$ 22 mm $\times$ 0.13 mm coverglasses, Catalog #12-542B, Fisher Scientific, Tustin, CA.

To prepare the holder for experiments, silicone vacuum grease (Dow Corning, Midland, MI) was applied to the lower inner surface to secure the coverslip (with device attached). The vacuum grease also functioned as a barrier to fluid leakage. This holder was then secured to the chuck of the Wentworth probe station and all four tungsten needle probes were placed in the square chamber, near the chip. A dummy piece of silicon, roughly 0.5 cm $\times$ 0.5 cm, was also placed in the corner of the chamber. This piece of silicon served as a blotting chip for the glue as well as a place to put the drop of cells far enough from

the device, but big enough to allow an adequate selection of cells.

Glue was then applied to the attachment sites, the chamber was filled with relaxing solution, and cells were added. Cell attachment and assembly of the microstructure then occurred, as described previously in Section III-E. The experimental chamber was usually rotated several times during the assembly sequence to get the probes in the optimal position for each step. After the structure was rolled off the edge of the wafer and cell slack was taken up, the sliders were glued to the substrate and the insert shown in Fig. 7 was placed in the square chamber.

H. Test Set-up and Imaging System

Cell experiments were conducted using a dedicated custom-made microscope and imaging system mounted on an air-suspension table. As shown in Fig. 8, the imaging system consisted of a 40$\times$ water immersion objective positioned underneath the experimental chamber and above a charge-coupled device (CCD) video camera. A selection of intermediate lenses (not shown) in the optical path between the objective and the camera allowed the magnification to be increased or decreased. The cell is visualized on a video monitor during the experiment, and images are recorded for later analysis (see below). Under typical conditions, the combined magnification from the microscope objective, intermediate lens, and video camera yielded a minimum spatial resolution of ± 0.3 μm as measured directly off the video monitor.

The holder with the device, insert, and attached cell was bolted down to a two-axis (x–y) micromanipulator, and the inverted lens could be raised and lowered (z–axis) for focusing. The cell was illuminated by a blue LED positioned above the experimental chamber. The light from the LED is transmitted through the cell into the objective lens, and the resulting image is captured by the CCD camera ("transmitted light illumination").
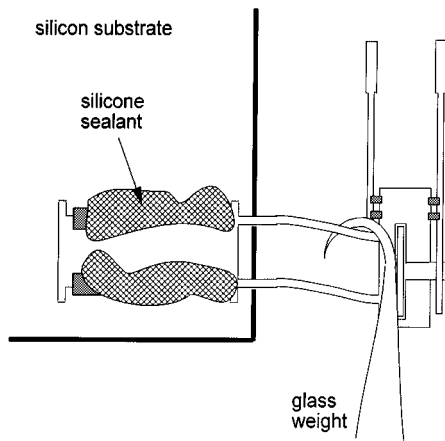
Fig. 9. Diagram of calibration of beams. Chip is mounted on a micromanipulator such that a glass weight can be hung from the beams. The beam deflection is optically measured to determine beam spring constant. Silicone sealant is used to secure the slider.

Activating and relaxing solutions could be selected by manually turning the valve and were pumped in manually through the input line. Instead of using the output line, a suction tube was placed at the top of the chamber to control the level of the solution meniscus [5]. By keeping the solution meniscus at a constant level, a steady focus of the cell image could be obtained. The suction tube was constructed from a glass rod and a gold mesh grid.[3] The grid was used to break the surface tension of the bath.

I. Image Analysis for Contractile Experiments

Cell images captured by the video camera were digitized using a PC-based frame-grabber system [16]. The digitized images were stored on an optical disk and were subsequently filtered, contrast enhanced, and analyzed on a pixel basis to obtain cell length and sarcomere striation pattern periodicity using custom software running on a VAXstation computer (Digital Equipment, Maynard, MA). At the relatively low magnification used for these studies, digital analysis yielded a spatial resolution of approximately ± 0.25 μm in the horizontal direction. Both the spacing between the clamps (cell length) and the sarcomere spacing were determined continuously during the experiments.

J. Beam Calibration

Beam calibration was performed on a horizontal axis video microscope system by hanging glass weights off the tips of the beams and measuring the resulting downward deflection, as shown in Fig. 9. The weights were made from thin glass tubing (glass standard 0.75 mm $\times$ 0.4 mm $\times$ 6 in, catalog #6255, A-M Systems Inc., Everett, WA). The glass was threaded through a heating coil and pulled to a fine point (about 5-μm tip diameter). The glass was then trimmed by breaking off bits at the wide end until a desired weight was attained. The weights used in the calibration ranged from 0.7–2.5$\pm$0.1 mg (1 mg $\approx$ 10 μN). The sharp tip was then fashioned into a hook by touching the tip to a plat-

inum heating wire under a stereomicroscope and bending the melted glass whisker that comes off. The weight of the polysilicon clamp at the end of the beams was negligible compared to the calibration weights used. Based on the calculated volume and density of silicon (2.3 g/cm^3 [17]), the estimated weight of the clamp was 0.23 μg.

The MEMS microstructure was assembled and secured to the substrate by applying silicone sealant over the base slider (Fig. 9). The chip was mounted on a glass coverslip for easy handling, with the device positioned far enough away from the edge that the weight did not interact with the coverslip edge. A separate horizontal optical axis microscope system was used to view the device as well as record the vertical deflection (a video camera was placed in one eyepiece). Illumination came through the back of the device, and the weights were placed at the tip of the beam using a suction tube attached to a separate three-axis micromanipulator. Suction was applied to the wide end of the weight (about 5–6 mm from the hooked end). Once the hook was positioned above the beams, the suction was removed and the weight fell on the beams. Deflection of the beams was recorded as well as the beam image after the weight was removed. The deflection was measured using video imaging software that recorded the number of pixels between marked points and converted to distance in microns (minimum resolution using this imaging method is ± 0.5 μm). In this case, the position of the beam tips with the weight on and off were marked. The video image was calibrated by imaging a calibration scale in which lines are separated by 100 μm (calibration slide made by Bausch & Lomb).

IV. RESULTS

During calibration, one of the beams would sometimes break due to improper weight handling or weight misplacement. Thus, beams could be calibrated individually as well as in pairs. For the single beams, the average spring constant over eight samples was 0.57$\pm$0.067 N/m. For the beams calibrated in pairs, the average spring constant over five samples was 1.47$\pm$0.36 N/m, which was roughly 2.5 times that calibrated for a single beam.

Force data from skinned heart cells were recorded during their response to activation solutions with various levels of calcium ion. Fig. 10 shows representative images of a cell during an experiment. The clamps, cell, and sarcomere striations were clearly visible in the relaxed state. In the contracted state, the cell's sarcomeres were less visible due to striations pattern nonuniformity and potential cell twisting. Such twisting most likely occurs during the cell manipulation step in the assembly sequence and is difficult to avoid. If the cell is not in the proper orientation when it was brought to the attachment sites, it has to be twisted around to fit.

The cell in Fig. 10 shortened roughly 19 μm in response to full activating solution ($\approx$23% of the cell's initial length). Given the calibrated spring constant of the two beams (1.47 N/m), and assuming half the total shortening occurs on either side, this cell generated about 14 μN of force. The average maximal force over seven cells was $F_{\max} = 12.6 \pm 4.66$ μN. These forces were comparable to those found by other groups studying the contractile characteristics of rat heart cells [3]–[5].
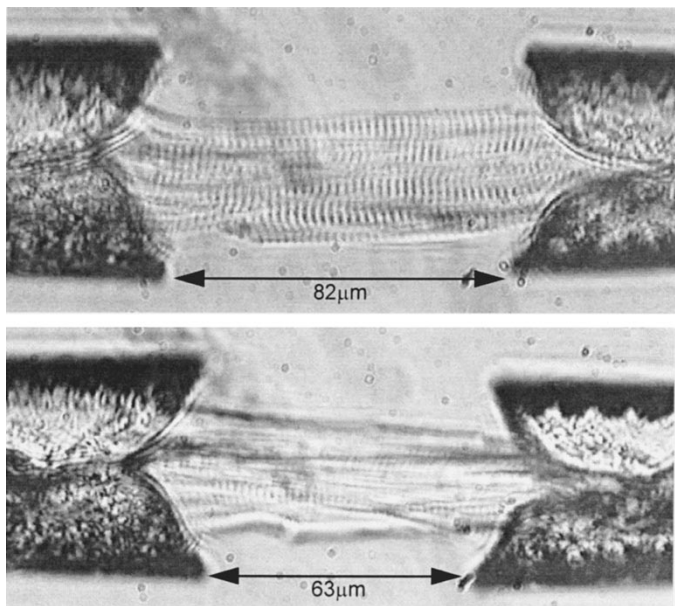
Fig. 10. Cell images during a contraction experiment. Cell on top is in relaxed state, image on bottom shows the same cell in a maximally contracted state in response to infusion of $pCa = 4.5$ solution. Based on the amount of shortening in the cell, $F_{\max} \approx 14\ \mu N$.
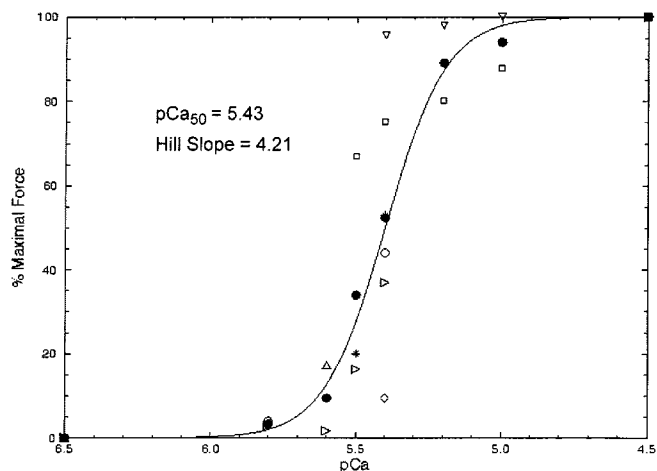

Fig. 11. Plot of percentage-maximal force versus increase in free calcium concentration from seven experiments. Fitted sigmoid curve is a plot of the Hill equation, in which $pCa_{50} = 5.43$ and Hill slope $= 4.21$ are the fitting parameters.

To normalize the force for different cell sizes, (2) was used to estimate the cross-sectional area of the cell. The width of each cell was measured and taken to be the minor axis of the ellipse. When the cell was first attached, it laid flat with the major axis in the plane of the substrate. This minor axis became visible when the cell was rotated $90°$ during clamp assembly. The average value obtained for $F_{\max}$/area was 23.7 ± 8.6 mN/mm^2. The average value agreed well with the 22.3 mN/mm^2 found using a standard commercial force transducer in a similar experiment (Cambridge 406A, Cambridge, MA) [5].

Using this device, intermediate forces were also resolved. Fig. 11 shows data from seven trials over a range of calcium concentrations (pCa). Using (3), the average data points were fit to a Hill curve. From the best fit sigmoidal curve, $n_H = 4.21$ and $pCa_{50} = 5.43$, which were comparable to the n_H and pCa_{50}

found in other laboratories [3]–[5]. Striation pattern image analysis determined that the sarcomere length of the cell in Fig. 10 was $1.99 \pm 0.13\ \mu m$ at rest and $1.65 \pm 0.25\ \mu m$ at maximal contraction. The average starting sarcomere length from seven trials was $1.99 \pm 0.04\ \mu m$ and the average maximally contracted sarcomere length $1.53 \pm 0.15\ \mu m$.

V. DISCUSSION

Sharpe *et al.* obtained an average measured value of 1.7×10^{11} N/m^2 for the elastic modulus of MUMP's polysilicon [18]. Using this value in (1), the theoretical spring constant of 0.68 N/m is fairly close to the 0.57 N/m measured value for a single beam. As mentioned in the theory section, the two beams together should have a combined spring constant eight times that of a single beam. Thus, the theoretical dual beam spring constant should be 5.44 N/m. The calibrated spring constant of 1.47 ± 0.36 N/m for the pair of beams was much lower than the theoretical value. Relatively large weights were used to produce measurable deflections in the beam pairs. It is possible that the silicone sealant used to glue the slider to the substrate exhibited some elasticity such that the slider rotated and produced a translation in the beams. Thus, the recorded deflection was larger than expected, and the beams appeared to be more flexible than theory predicted. This may also explain the discrepancy between theoretical and measured values for the single-beam spring constants.

During cell experimentation, the force was generated at the end of the clamp. Thus, there may be some calibration error due to placing the weights at the end of the beam rather than at the end of the clamp where force was actually generated. The polysilicon plates that hold the cell were attached to the beams via scissor hinges. Since there were only a few micrometers of slack in the hinges in the direction of force generation, the clamp can be treated as a solid mass at the end of the beams. Furthermore, the weight of the polysilicon clamp was practically negligible ($0.23\ \mu g$). Thus, the calibration error due to loading the beams at the tip rather than at the end of the clamp for calibration should be minimal.

In terms of force generation, an isometric contraction at starting sarcomere length of $1.99\ \mu m$ should produce maximum force since the contractile filament overlap is optimal [2]. However, in a true isometric contraction, the length of the cell is fixed. This was clearly not the case in this design since the beams had to be very flexible to produce enough deflection for a visual readout. A sarcomere length of $1.53\ \mu m$ is physiologically very short for striated muscle. With the cell length fixed, the cell would develop force in a more physiologically correct configuration, but this was not possible with this design.

Furthermore, the experimental methods (cell manipulation with probes, gluing, and clamping) may have some physiological effect on the cell ends and their functionality. Disruption of some of the contractile filaments likely occurred at the cell ends. Since the topology of the cell ends varied from cell to cell, the amount of disruption will be difficult to quantify. However, the central portion of the cell visible between the clamps was untouched by probes or glue. Image analysis indicated no cell damage or sarcomere disruption between the clamps in resting

cells. Activated cells contracted strongly. Thus, any potential cell end damage did not significantly effect the experiment.

Though no oscillatory or length transient data were obtained with this device, linear beam theory predicts a resonant frequency of at least 13 kHz, using the calibrated spring constant of the beam pair (1.47 N/m) and the mass of each structure (0.23 μg = beams + clamp). This bandwidth is more than adequate for complex stiffness modulus measurements (stiffness/area) via longitudinal cell oscillations [1], [5]–[7] or for force or length transient studies on cells [3], [4], [9]. To achieve this goal, the next step would be to integrate an actuator to drive the clamp. Electrostatic and thermal actuators have both been demonstrated in the MUMP's process [19], [20]. However, electrostatic operation in solution may be difficult, and thermal actuation may be inappropriate near a living cell since the operation temperature often exceeds 100 °C. Magnetic actuation may be a viable alternative, as it has been demonstrated to operate in solution [21]. However, magnetic actuation using the MUMP's process will require the integration of post-processed magnetic materials.

When this device was developed, MUMP's did not support integrated electronics (they now support a hybrid technology involving indium bump bonding of a CMOS chip). The visual deflection readout limited the force resolution and required substantially more beam compliance than desirable for optimal force determination from the cell. Although this polysilicon device clearly demonstrates the feasibility of MEMS-based force transduction from cells, improvements are necessary for routine measurement. Ideally the beams would be very stiff and voltage data from a strain gauge would be recorded on a PC in real time. Force development transients and high-frequency oscillation data can reveal critical molecular events during force generation. To address these issues, a standard CMOS version of this cell force transducer was developed concurrently, which incorporated strain gauges and some simple signal-processing electronics [22]. Although some force results were obtained, this version is still under development.

VI. CONCLUSIONS

With this commercially fabricated surface-micromachined cell force transducer, force has been measured from single heart cells. Cells were attached to a MEMS transducer, while submersed in a nutrient saline solution, and they were imaged with a digital-imaging microscope system. Cell attachment occurred simultaneously with device assembly. The initial measurements of steady-state force (F_{max}, F_{max}/area, n_H, and pCa$_{50}$) were comparable to those measurements from other laboratories using standard force transducer technology. Clearly, MEMS-based force transduction from heart cells can be achieved. However, with the appropriate enhancements such as strain gauge and microactuator integration, MEMS force transducers offer the capability of high-resolution dynamic readings of contractile force development in isolated cardiac myocytes and other contractile cells at a greater fidelity than previously attainable.

REFERENCES

[1] M. Kawai, Y. Saeki, and Y. Zhao, "Crossbridge scheme and the kinetic constants of elementary steps deduced from chemically skinned papillary and trabecular muscles of the ferret," *Circulation Res.*, vol. 73, pp. 35–50, 1993.

[2] K. P. Roos, "Mechanics of force production," in *The Myocardium*, 2nd ed, G. A. Langer, Ed. New York: Academic, 1997, ch. 6, pp. 235–323.

[3] A. Araujo and J. W. Walker, "Kinetics of tension development in skinned cardiac myocytes measured by photorelease of Ca^{2+}," *Amer. J. Physiol.*, vol. 267, pp. H1643–H1653, 1994.

[4] P. A. Hofmann and J. H. Lange, "Effects of phosphorylation of troponin I and C protein on isometric tension and velocity of unloaded shortening in skinned single cardiac myocytes from rats," *Circulation Res.*, vol. 74, no. 4, pp. 718–726, Apr. 1994.

[5] R. E. Palmer, A. J. Brady, and K. P. Roos, "Mechanical measurements from isolated cardiac myocytes using a pipette attachment system," *Amer. J. Physiol.*, pp. C697–C704, 1996.

[6] K. P. Roos and A. J. Brady, "Stiffness and shortening changes in myofilament extracted rat cardiac myocytes," *Amer. J. Physiol.*, vol. 256, pp. H539–H551, 1989.

[7] ——, "Osmotic compression and stiffness changes in relaxed skinned rat cardiac myocytes in PVP-40 and Dextran T-500," *Biophys. J.*, vol. 58, no. 5, pp. 1273–1283, Nov. 1990.

[8] N. K. Sweitzer and R. L. Moss, "The effect of altered temperature on Ca^{2+}-sensitive force in permeabilized myocardium and skeletal muscle. Evidence for force dependence of thin filament activation," *J. Gen. Physiol.*, vol. 96, no. 6, pp. 1220–1245, Dec. 1990.

[9] M. R. Wolff, K. S. McDonald, and R. L. Moss, "Rate of tension development in cardiac muscle varies with level of activator calcium," *Circulation Res.*, vol. 76, pp. 154–160, 1995.

[10] M. Fauver, D. L. Dunaway, D. H. Lilienfeld, and H. G. Craighead, "Microfabricated cantilevers for measurement of subcellular and molecular forces," *IEEE Trans. Biomed. Eng.*, vol. 25, pp. 891–898, July 1998.

[11] K. S. J. Pister, M. W. Judy, S. R. Burgett, and R. S. Fearing, "Microfabricated hinges," *Sens. Actuators*, vol. 33, no. 3, pp. 249–256, 1992.

[12] G. Lin, K. S. J. Pister, and K. P. Roos, "Novel microelectromechanical system force transducer to quantify contractile characteristics from isolated cardiac muscle cells," *J. Electrochem. Soc.*, vol. 142, no. 3, pp. 631–633, 1995.

[13] ——, "Micro-scale force transducer system to quantify isolated heart cell contractile characteristics," *Sens. Actuators*, vol. 46, no. 1/3, pp. 233–236, 1995.

[14] P. B. Chu, P. R. Nelson, M. L. Tachiki, and K. S. J. Pister, "Dynamics of polysilicon parallel-plate electrostatic actuators," *Sens. Actuators*, vol. 52, pp. 216–220, 1996.

[15] G. Lin, K. S. J. Pister, and K. P. Roos, "Heart cell contractions measured using a micromachined polysilicon force transducer, in micromachined devices and components," *Proc. SPIE*, vol. 2642, pp. 130–137, 1995.

[16] K. P. Roos and S. R. Taylor, "High-speed video imaging and digital analysis of microscopic features in contracting striated muscle cells," *Opt. Eng.*, vol. 32, no. 2, pp. 306–313, Feb. 1993.

[17] K. E. Petersen, "Silicon as a mechanical material," *Proc. IEEE*, vol. 70, pp. 420–457, May 1982.

[18] W. N. Sharpe Jr., B. Yuan, and R. L. Edwards, "A new technique for measuring the mechanical properties of thin films," *J. Microelectromech. Syst.*, vol. 6, pp. 193–199, Sept. 1997.

[19] R. Yeh, E. J. J. Kruglick, and K. S. J. Pister, "Surface-micromachiined components for articulated microrobots," *J. Microelectromech. Syst.*, vol. 5, pp. 10–17, Mar. 1996.

[20] J. H. Comtois, V. M. Bright, and M. W. Phipps, "Thermal microactuators for surface-micromachining processes," *Micromachined Devices Comp.*, vol. 2642, pp. 10–21, 1995.

[21] J. W. Judy, R. S. Muller, and H. H. Zappe, "Magnetic microactuation of polysilicon flexure structures," *J. Microelectromech. Syst.*, vol. 4, pp. 162–169, Dec. 1995.

[22] G. Lin, R. E. Palmer, K. S. J. Pister, and K. P. Roos, "Single heart cell force measured in standard CMOS," in *9th Int. Solid-State Sens. Actuators Conf.*, Chicago, IL, June 16–19, 1997, pp. 199–200.

Kristofer S. J. Pister received the B.A. degree in applied physics from the University of California at San Diego, in 1982, and the M.S. and Ph.D. degrees in electrical engineering from the University of California at Berkeley, in 1989 and 1992, respectively.

In 1992, he became an Assistant Professor of electrical engineering at the University of California at Los Angeles, where he developed three graduate-level courses in MEMS systems: MEMS device physics and fabrication, MEMS design, and computer-aided design (CAD) for MEMS. In 1996, he joined the faculty of electrical engineering and computer sciences at the University of California at Berkeley, where he is currently an Associate Professor. During the last five years, his primary research interest has been the development and use of standard fabrication technologies, general-purpose design paradigms, and CAD for MEMS. Some of the applications of his research include micro robotics, micro optics, and distributed sensor networks. He is an active consultant in the MEMS industry, and holds two patents on MEMS technology and applications.

Gisela Lin (S'89–M'92) received the Ph.D. degree in electrical engineering from the University of California at Los Angeles, in 1998, the M.S. degree in electrical engineering from the University of California at Santa Barbara in 1992, and the B.S. degree in electrical engineering and material science engineering from the University of California at Berkeley in 1990.

She is currently with the Jet Propulsion Laboratory, Pasadena, CA, where her research focuses on MEMS biosensor packaging, which includes microfluidic handling, liquid sample acquisition, and biocompatible materials characterization. She is also involved in the development of miniature liquid chromatographs and microfluidic circuits for extraterrestrial soil sample analysis.

Kenneth P. Roos received the Ph.D. degree in zoology from the University of California at Davis, in 1978, and the M.S. degree in biology from San Diego State University, San Diego, CA, in 1974, and the A.B. degree in applied physics and informational science from the University of California at San Diego, in 1971.

Since 1978, he has been with the Cardiovascular Research Laboratory and the Department of Physiology, University of California at Los Angeles (UCLA) School of Medicine. He is currently an Adjunct Professor. His research centers on the biophysics of cardiac muscle contraction in cardiomyopathic heart.